Flavon-based chemosensor: A host-guest interaction analysis of hydroxyl group with cyanide anion

Cite as: AIP Conference Proceedings **2609**, 020004 (2023); https://doi.org/10.1063/5.0123594
Published Online: 02 March 2023

R. Rahmawati and Saprizal Hadisaputra

Flavon -Based Chemosensor: A Host-Guest Interaction Analysis of Hydroxyl Group with Cyanide Anion

R. Rahmawati, Saprizal Hadisaputra[a)]

Chemistry Education Division, Department of Mathematics and Natural Sciences Education, Faculty of Teacher Training and Education, Universitas of Mataram, Mataram, Indonesia.

[a)] *corresponding author: rizal@unram.ac.id*

Abstract: The S8 flavon-based sensor has been successfully synthesized. The testing on the activity of S8 as a sensor for anions that have been carried out on cyanide anion. Analysis of the S8 host-guest interaction with CN ion ions was qualitatively performed using UV-Visible, NMR proton spectra resulting from titration of S8/DMSO solution with CN^- ions. The density functional study provides information about the mechanism of the sensor between the S8 and the CN- anion. analysis showed that the hydrogen bond between the hydroxyl group on the S8 and the CN^- ion did not deprotonate from S8 to the CN^- ion.

INTRODUCTION

Anions play a fundamental role in many chemical processes to result in increased attention, specifically in recognizing and detecting anionic species. Many attempts have been made to design chemical sensors that make it possible to produce selective anion detectors visually and quantitatively. Simple sensors can produce discoloration with the presence of anions in various organic solvents [1].

The sensor is a system that can experience intermolecular interactions with an analyte and produce stimulants due to changes in energy from lower levels to higher levels or vice versa. The interaction will result in changes in electronic properties to the signal side, followed by changes in color, fluorescence, or electrochemistry in the system [2].

Two essential components of chemosensor design are signal-site (fluorophore or chromophore) and recognition-site (receptors). Signal-site acts as a transducer that converts information (recognition events) into optical responses. Recognition-site is responsible for selectively and efficiently engaging with analytes. The ability of sensors to detect analytes depends on the ions' character and the sensor's molecular structure while still considering solvent factors, pH, ionic strength, and polarity [3].

Anion detection is not only an anion binding activity in the form of interactions involving non-covalent bonds only, but also like hydrogen bonds or deprotonation, the main interactions occur in protons from the -OH or -NH binding side [4]. Interactions that occur on the bonding side of the sensor with anion determine the selectivity and sensitivity of the sensor to anions. The sensor interaction with anions is influenced by the nature of the anion [5] and the solvent system [6,7].

Chemosensors based on optical properties have been used as cation sensors, anions, and neutral compounds called optical sensors. Optical sensors can be divided into two: chromogenic chemosensors and fluorogenic chemosensors. A chromogenic chemosensor is a chemosensor where the interaction between the binding site and the analyte results in the signal unit showing color changes while fluorogenic chemosensors are the type in which the coordination that occurs due to the interaction of the binding side with the analyte results in the signal side showing fluorescent changes [3].

In the process of recognizing sensor-specific interaction with the analyte, several photochemical mechanisms can be used, namely ICT (intermolecular charge transfer) and PET (photoinduced electron transfer). PET is based on the principle that in an excited state, the oxidative-reductive properties of a molecule increase, and the electron transfer

The 6th International Conference on Science and Technology (ICST21)
AIP Conf. Proc. 2609, 020004-1–020004-7; https://doi.org/10.1063/5.0123594
Published by AIP Publishing. 978-0-7354-4335-8/$30.00

process occurs. Receptor units are electron donors, and fluorophore units are electron receivers connected by carbon chains [8].

The recognition process of most analytes is a sensor-ion interaction (host-guest interaction) based on the selectivity of host-guest complexation reactions. The interaction style of this process can be ion-dipole, dipole-dipole, and interaction-interaction [9]. The relationship between the sensor and the analyte can be seen as the interaction of the formation of a complex system of qualitative and quantitative host-guest chemosensors. The interpretation can be viewed mathematically from (a) quantitative complex formation (determination of kass) and; (b) recognition quality (determination of detection limits). The calculation method is used as a criterion for evaluating the process of host-guest interaction based on its concentration. This method can be determined from UV-vis and 1H-NMR titration data [10].

Therefore, the analysis was performed using H-NMR titration spectra data to signaling sensor interactions with the analyte via hydrogen bonds [11]. The 1H-NMR titration method strongly indicates the binding of anions (anion binding) because the addition of ions results in hydrogen bonds between host-guests characterized by the loss of the proton sensor's resonance signal to deprotonation [12]. The strength of host-guest bonds in the complex sensor-anion system comes from hydrogen bonds and π-π interactions [13]. Sensors from the flavon group (called S8) that we have synthesized in this project will be analyzed qualitatively on how the effect of the bonds between the hydroxyl groups of the connective groups on the sensor with the CN ions to the proton-proton sensor compounds due to the induction of the electron bond π.

METHODOLOGY

Materials

All reagents for synthesis obtained commercially were used without further purification, DMSO, and aquadest. The anions were added in the form of sodium cyanide (NaCN salt).

Experimental procedure

The concentration of the sensor solution used is based on the initial test results, which was the sensor concentration that showed the optimal absorbance on the UV-Vis measurement. A total of 3.2 mg of S8 was dissolved in 120 mL DMSO so that the concentration of the S8 / DMSO solution became 1×10^{-7} M. As much as 3 mL of the solution was put into three series vials for titration treatment, namely: vial 1, blank, 0 eq., sensor solution without the addition CN ions; vial 2, is three ek., the sensor solution with the addition of 50 µL CN ions 2×10^{-9} M; and vial 3, is eight ek., a sensor solution with the addition of 50 µL CN^- ions 5×10^{-9} M. Then the resolution of the three vials was analyzed by the proton shift spectra using a ^{1}H-NMR instrument. The titration analysis using the 1H-NMR instrument was carried out to quantitatively identify the S8-CN^- host-guest interaction that occurred between the hydroxyl group from the connective side of the S8 chemosensor with the CN ions to see the tendency of proton shifts after the interaction occurred. ^{1}H NMR was measured using a JOEL JNM ECA-500 MHz; fluorescent were measured using a Shimadzu RF-6000 Spectro Fluorophotometer.

Computational Studies

The optimization of the S8 structure was carried out using the DFT method at the theoretical level in B3LYP/6-31G(d). All geometric calculations were carried out using Gaussian 09 [14]. The effect of solvent was measured using a continuum solvation model approach. The dielectric constant in the solution follows the default of Gaussian 09.

RESULT AND DISCUSSION

The synthesis of the S8 compound was carried out by heating chalcone in DMSO solvent with an iodine catalyst at the solvent's boiling temperature. The synthesis scheme is presented in Fig. 1.

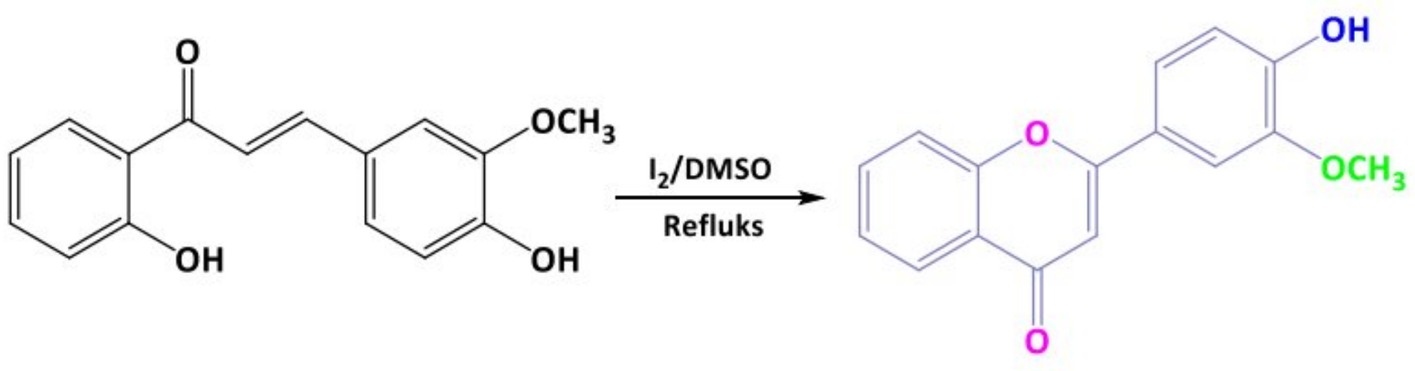

FIGURE 1. S8 synthesis of chalcones

Confirmation of the structure of the synthesized product was also carried out with a ^{1}H-NMR spectrometer whose spectra are presented in Fig. 2. OH protons and two alkene protons from chalcones that appear on δ 16.47 ppm, 7.60 ppm, and 8.06 ppm, respectively, disappear from the spectra. They were replaced by protons from the flavon ring (Hc) on the ring δ 6.69 ppm and benzene ring protons from cyclic fused (Hh), which experience downfield from 6.96 ppm to 8.04 ppm. The O-H proton from the chalcone phenol ring that appears at δ 3.83 ppm experiences downfield to δ 9.94 ppm at S8.

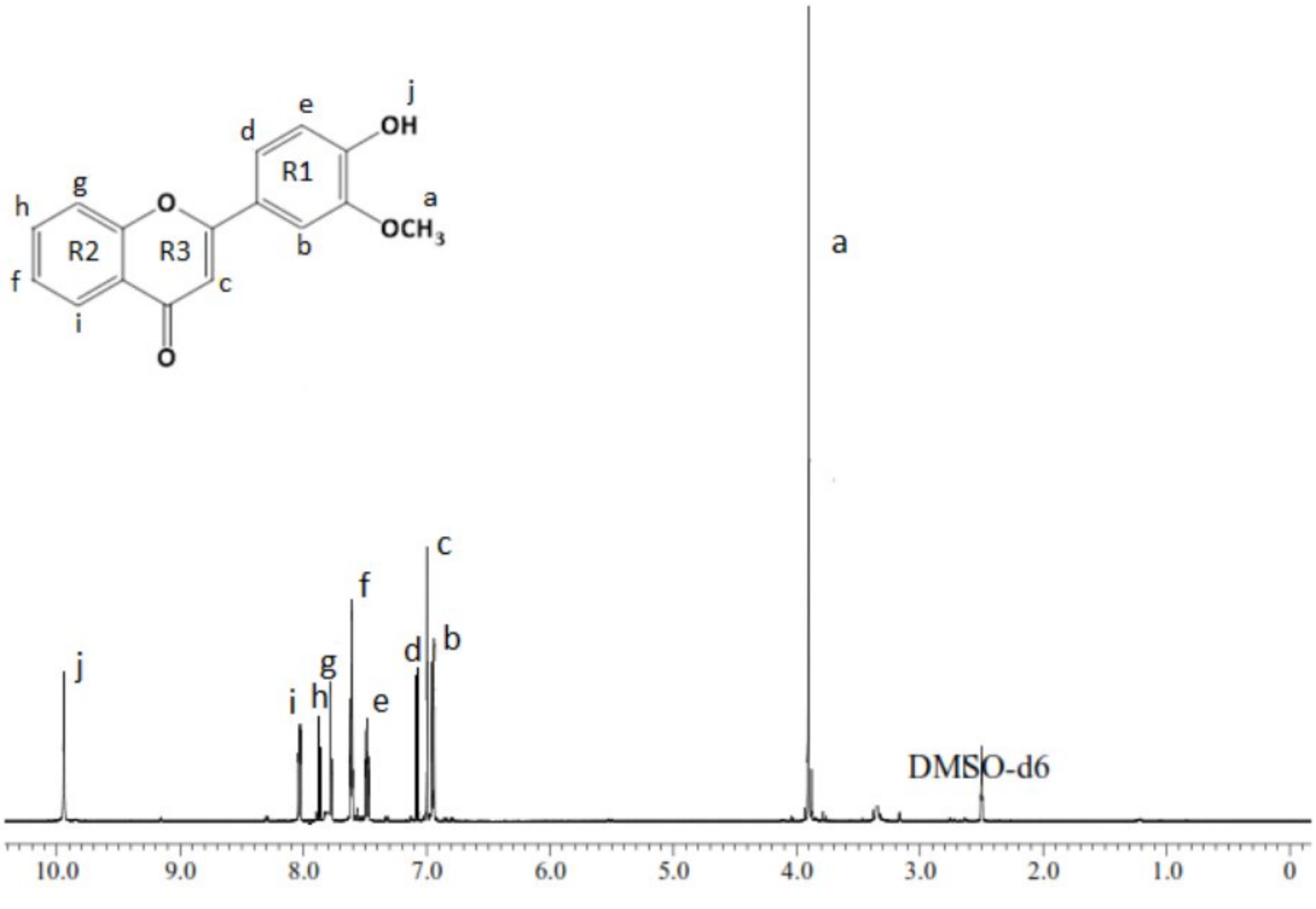

FIGURE 2. 1H-NMR spectrum of S8 synthesized from chalcone.

Observation under UV light 366 nm showed fluorescent in S8 solution without anion (fluorescent 'on'), and fluorescent was also observed in S8 solution added with ions of CN ion and F^- (fluorescent 'on'). Therefore, S8 is a dual sensor, a selective color sensor for CN^- ions, and an "on-on" fluorescent sensor for CN^- ions.

Qualitative analysis of the titration of the S8 / DMSO solution with CN^- ions was performed by UV-Vis spectroscopy, and the measured spectra are shown in Figure 3b. Without CN ions, the S8 solution absorbs at λ 331 nm (A value is 1.4) with the shoulder at λ 441 nm. The addition of 5×10^{-7} M (ek. 1) CN^- ions results in decreased absorbance and absorbance in the shoulder being increased, indicating that there has been an electron transition π-π* from chromophores. The decrease in absorbance at λ 331 nm continues until the addition of $5 \times 10^{-}4$ M (ek. 8) is followed by the continued increase in absorbance at λ shoulder (441 nm) due to the n-π* transition. At the same time, an isosbestic point is formed at λ 370 nm [15]. A bathochromic shift of 109 nm that occurred and an isosbestic point formed showed an interaction between S8 and CN^-, forming one type of active complex, S8-CN^- [16].

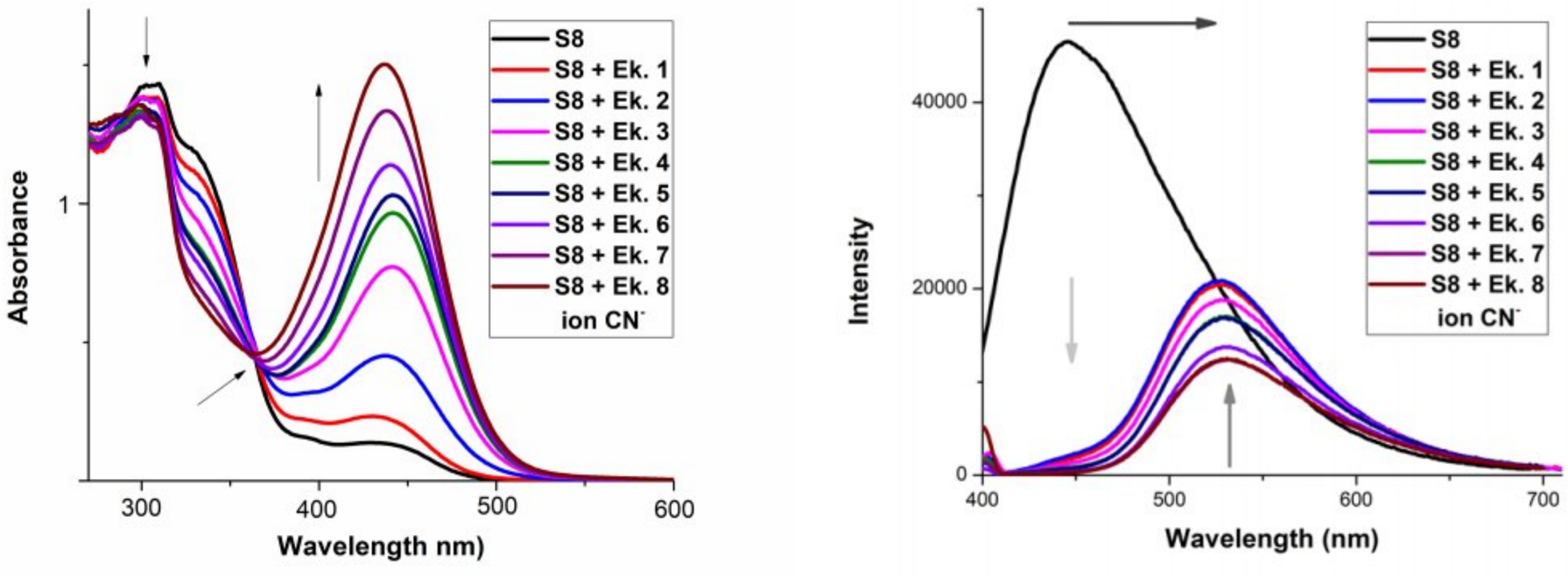

FIGURE 3. (a) UV-Vis titration spectra of S8 with CN^- ions; (b) S8 fluorescent titration emission spectrum of S8 with CN^- ions.

Fluorescent S8 compounds are light blue, with fluorescent color CN^- ion ions becoming thicker (deep blue) and fluorescent color, F ions turning greenish. The addition of CN dan and F^- ions with a concentration of 5×10^{-7} M (ek. 1) to a concentration of 5×10^{-4} M (ek. 8) gradually produces a stronger intensity of fluorescent color. On the addition of F^- ions, the greeny fluorescent color on the addition of 5×10^{-7} M (ek. 1) ions to greeny-yellow addition of 5×10^{-4} M (ek. 8). Quantitative analysis of the interaction of the host-guest complex S8 CN^- is done by measuring fluorescence intensity using a spectrophotometer instrument. The spectra of the measurement results are shown in Figure 3a, without the CN^- S8 ion excitation at λ 420 nm and emission at λ 445 nm with an intensity of 425000. The addition of 5×10^{-7} M (ek. 1) to 5×10^{-4} M (ek. 8) CN^- ions causes the displacement of λ excitation of the S8-CN^- complex to λ 440 nm, and emission shifted to λ 525 nm so that a redshift occurs with a stoke's shift value of 80 (Fig. 3b).

The stoke's shift formed on the titration with CN^- indicates the occurrence of PET processes in the S8-ion complex [17,18]. Quantitative analysis of the formation of the S8-CN^- host-guest complex gives a k_{ass} value of the S8-CN^- complex is 1×10^5 M^{-1}. The calculation of the stoichiometric ratio determines the analysis of the S8-CN^- complex host-guest interaction model. The interaction of the S8-CN complex in UV-Vis titration reaches a maximum absorbance value when frimimol is 0.5. The fractionimol 0.5 indicates that host-guest interaction occurs when the S8/CN^- stoichiometric ratio is 1: 1. [19,20]. It's mean: the interaction model occurs through the formation of hydrogen bonds by protons on the connective side of the -OH group of 1 S8 molecule with electrons from 1 molecule of CN^- ion ions, so that the signal side responds in the form of complex color changes and increased fluorescent complexes. The proposed interaction model of each stoichiometric ratio is shown in Fig. 4.

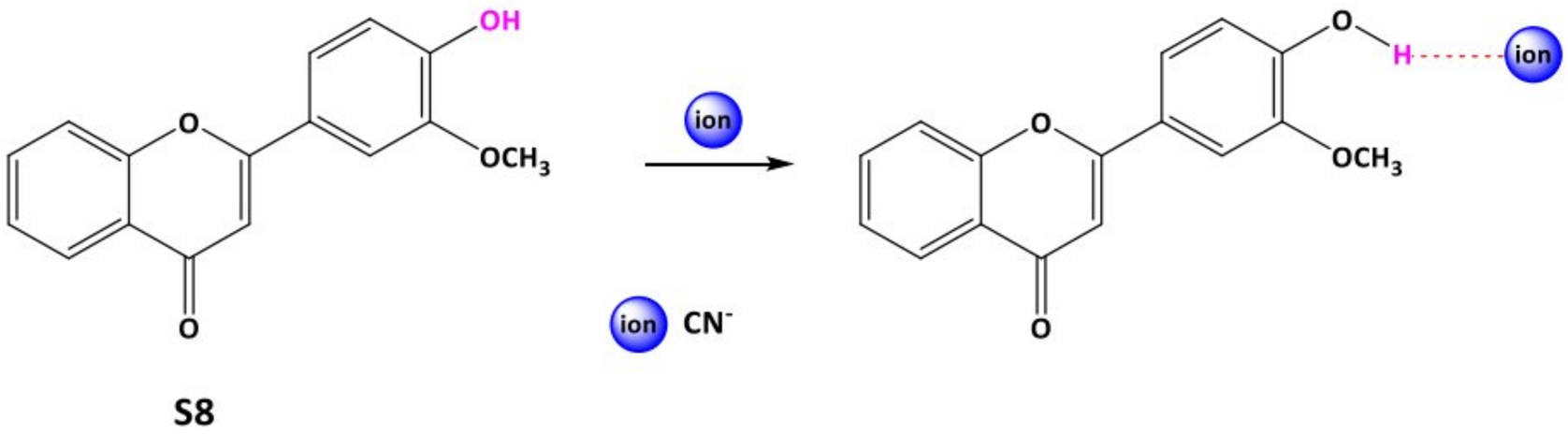

FIGURE 4. Analysis of S8-CN^- host-guest titration with 1H-NMR

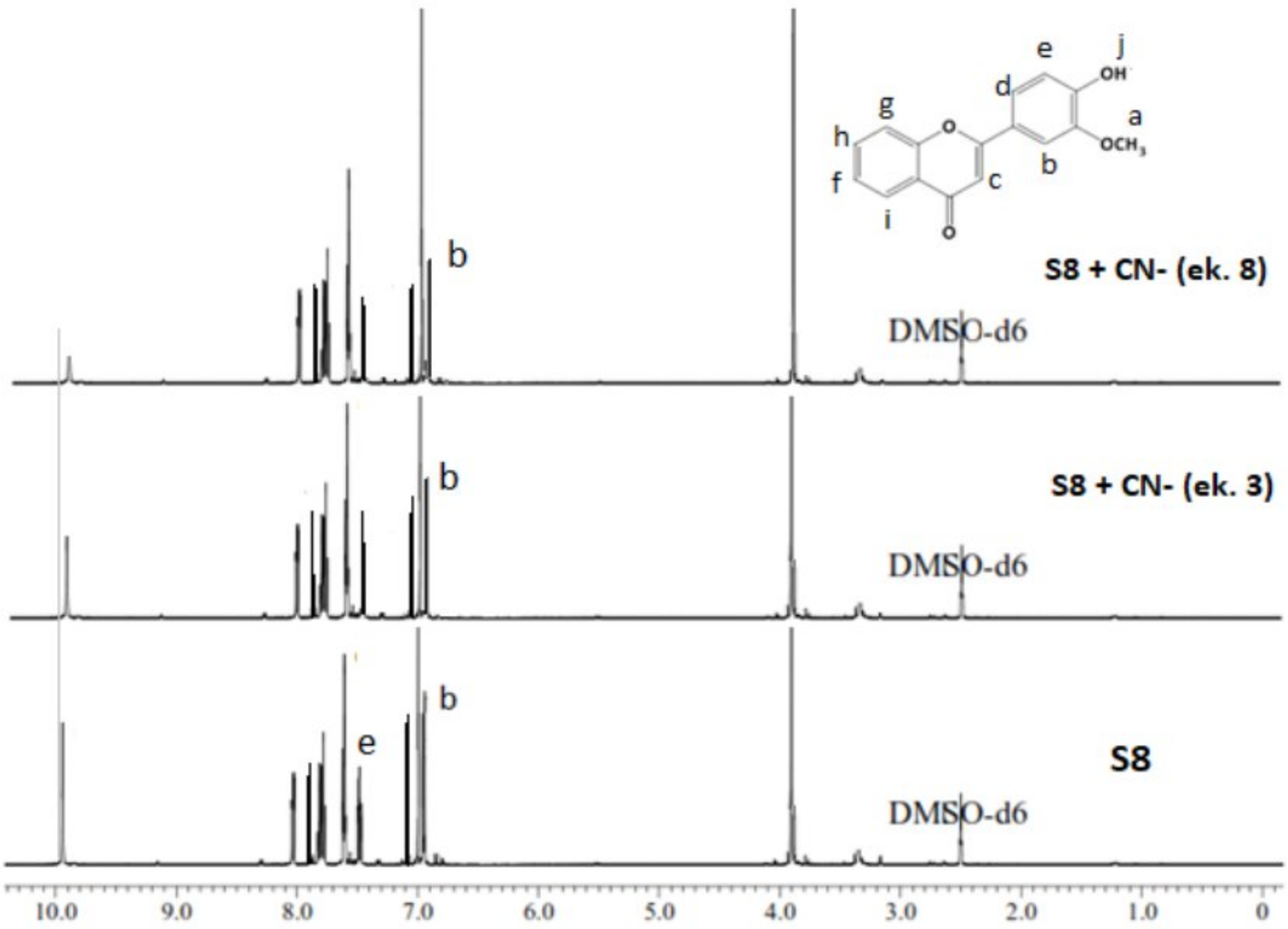

FIGURE 5. ^{1}H-NMR spectrum of S8 titration with CN^- ions

Titration analysis using the ^{1}H-NMR instrument was carried out to see the host-guest bonding process between S8 and CN^- ions on the connective side of the -OH group. Measurement of 1H-NMR on titration with CN^- equivalent ions. 0 ek., ek. 3, and ek. 8. Spectra results of the analysis with 1H-NMR are presented in Fig. 5.

Proton (H) -OH group of S8 without the presence of CN^- ions shows a peak at δ 9.94 ppm. As a gradual addition of CN^- ions, the intensity of the peak Hh (proton –OH) decreases until the addition of 5×10^{-4} M (ek. 8) peaks intensity almost disappears. It shows that there is a strong interaction of ions with protons through hydrogen bonds [15]. At the same time, the aromatic protons experienced a gradual upfield shift, the Hd shifted from 7.49 ppm to 7.30 ppm, and the Hb shifted slightly from 6.94 ppm to 6.90 ppm. Load delocalization occurs due to shifting upfield Hb and He [21,22]. The density of electrons in the phenyl ring that occurs through the propagation of hydrogen bonds and the resulting shielding effect results in an upfield shift in aromatic protons [23]. No triplets formed at δ above 10 ppm indicated no deprotonation in the S8 host-guest interaction with CN^- [20].

Computational Study of S8 with Cyanide Anion.

We performed density functional analysis using the Gaussian 09 with B3LYP/6-31G(d) to investigate the nature of the sensing mechanism between S8 and CN^-. The ground-state geometry optimizations and excited-state electronic transitions were performed first in the gas phase, followed by geometry optimization in the solvent phase. To accomplish this, a solvent model was used, with dimethylformamide as the solvent for the ground and excited-state calculations using DFT-B3LYP. In free receptors and their receptor CN complexes, the geometries and orientation of the highest occupied molecular orbital (HOMO) and lowest unoccupied molecular orbital (LUMO) have been optimized. The lowest unoccupied molecular orbital (LUMO) is 1.807 eV in S8, and the highest occupied molecular orbital (HOMO) (5.870 eV). The bandgap of the optimized structure in the gas phase is 4.07 eV. The presence of anion induction at the receptor in the solution phase reduces the bandgap from 4.07 eV to 3.16 eV. It gives a redshift band in the observed UV-VIS spectrum. The redshift shape change indicates that the anion is bound to the receptor (Figure 6) [24].

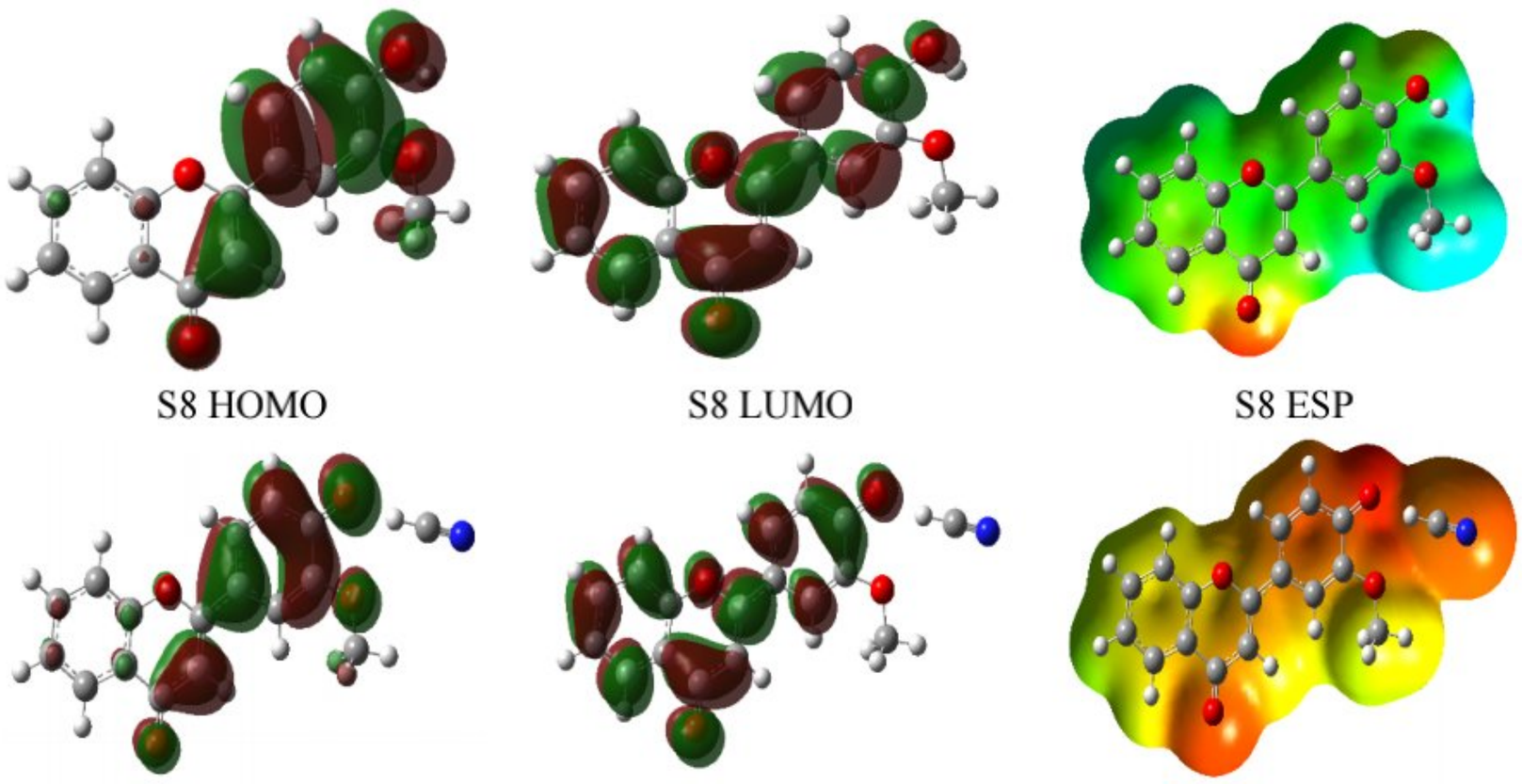

FIGURE 6. Visualization of the highest occupied molecular orbital (HOMO), the lowest unoccupied molecular orbital (LUMO) and the electrostatic surface potential (EPS) of S8 and its CN^- complex.

CONCLUSION

In conclusion, the S8 has successfully synthesized as a chemosensory for CN- in an aqueous solution. A change in the fluorescence intensity was observed after adding cyanide to the S8 probe in an aqueous medium. DFT study shows reduced bandgap after CN^- was detected. Based on NMR proton spectra, S8 host-guest interaction with CN ions does not indicate the deprotonation process has occurred. Only the strong interaction of ions with protons occurs through hydrogen bonds.

REFERENCES

1. C. R. Nicoleti, V. G. Marini, L. M. Zimmerman, V, G. Machado, J. Braz. Chem. Soc., **22,** 8, 1488-1500, (2012).
2. O. Sahin, M. Sahin, N. Kocak, M. Yilmaz, Turk. J. Chem., **37**, 832-839 (2013).
3. B. Wang, E. V. Anslyn, Chemosensor : Principles, Strategies, and Applications, A John Wiley & Sons (2011).
4. V. Reena, S. Suganya, S. Velmathi, J. Fluorine Chem., **153,** 89-95, (2013).
5. D. Sharma, R. K. Bera, S. K. Sahoo, Spectrochimia Acta Part A., **105,** 477-482 (2013).
6. J. Kang, e. J. Song, H. Kim, Y-H. Kim, Y. Kim, S-J. Kim, Tetrahedron Letters, **54,** 1015-1019 (2013).
7. H. Nie, C. Gong, Q. Tang, X. Ma, C. Chow, Dyes Pigm., **106,** 74-80 (2014).
8. A. J. C. Moro, Design of Fluorescent Chemosensor for Naproxen and ATP and Subsequent Immobilization in Nanoparticles, Dissertation, Schiller-Universitat Jena, (2010).
9. A. Dybko, W. Wroblewski, Pol. J. Environ. Stud., **11**, 5-10 (2002).
10. K. Hirose, J. Incl. Phenom. Macrocycl. Chem., **39**, 193-209 (2001).
11. R. Rahmawati, S. W. Al Idrus, S. Supriadi, L.Sulman, L. Acta Chim Asiana, **4**, 1, 104-107. (2021).
12. Udhayakumari, D., Velmethi, S., Chen, W-C., dan Wu, S-P., Sens. Actuators B, **204**, 375-381 (2014).
13. Razi, S. S., Srivastava, P., Ali, R., Gupta, R. C., dan Dwivedi, S. K., Sens. Actuators B, **209**, 162-171 (2015).
14. A. Frisch. gaussian 09W Reference. *Wallingford, USA, 25p*. (2009)
15. A. Singh, S. K. Sahoo, D. R. Trivedi, Spectrochim. Acta A, **188**, 596-610 (2018).
16. A. Singh, S. Tom, D. R. Trivedi, J. Photochem. Photobio A: Chem, **353**, 507-520 (2018).
17. J. Qin, T. Li, B. Wang, Z. Yang, L. Fan, Synthetic Metals, **195**, 141-146 (2014).
18. R. Rahmawati, S. W. Al-Idrus, B. N. Sari, B. Purwono, S. Acta Chim Asiana, **3**, 1, 143-146 (2020).
19. P. Gholamzadeh, G. M. Ziarani, N. Lashgari, A. J. Badiei, Fluorescence, **26**, 1857-1864 (2016).

20. J. Tan, X. Wang, Q. Zhang, H. Zhou, J. Yang, J. Wu, J. Tian, X. Zhang, Sens. Actuators B, **260**, 727-735 (2018).
21. P. Srikala, K. Tarafder, D. R. Trivedi, Spectrochim. Acta A., **170**, 29-38 (2017).
22. R. Rahmawati, B. Purwono, S. Matsjeh, Acta Chimica Asiana, **2**, 2, 110-113 (2019).
23. Y. K. Tsui, S. Devaraj, Y.P. Yen, Sens. Actuators B, **161**, 510-519 (2012).
24. O. Dalkilic, F. Lafzi, H. Kilic, N. Saracoglu. Tetrahedron Lett, **61,** 37, 152315. (2020).